Table 3. Summary statistics for total particle number concentrations (D_{p}>15 nm; N_{tot}) and for concentrations of particles in three size-ranges typical for CCN; D_{p}>50 nm (N_{50}), >100 nm (N_{100}) and >160 nm (N_{160}). The normalised mean bias (NMB), slope of the linear regression (m) and correlation coefficient (R^2) are calculated between the simulated and observed multi-site campaign-mean number concentrations.

Model	NMB (%)				m				R^2			
Experiment	N_{tot}	N_{50}	N_{100}	N_{160}	N_{tot}	N_{50}	N_{100}	N_{160}	N_{tot}	N_{50}	N_{100}	N_{160}
BCOC_lg	−68	−52	−29	−1	0.23	0.44	0.64	0.74	0.64	0.82	0.86	0.71
BCOC_sm	−28	−18	−1	9	0.73	0.80	0.81	0.65	0.71	0.86	0.77	0.47
ACT-BCOC_lg	−53	−43	−22	−1	0.24	0.44	0.65	0.75	0.68	0.87	0.83	0.69
ACT-BCOC_sm	−19	−13	4	10	0.71	0.82	0.83	0.67	0.72	0.86	0.76	0.49
KIN-BCOC_lg	−43	−38	−19	−1	0.26	0.45	0.66	0.74	0.63	0.88	0.81	0.71
KIN-BCOC_sm	−13	−11	6	9	0.70	0.80	0.84	0.67	0.71	0.87	0.77	0.49
ORG1-BCOC_lg	−40	−37	−17	<1	0.22	0.45	0.68	0.73	0.35	0.87	0.82	0.65
ORG1-BCOC_sm	−11	−11	7	8	0.67	0.81	0.86	0.65	0.66	0.87	0.77	0.48
ORG2-BCOC_lg	−46	−40	−20	<1	0.25	0.44	0.74	0.70	0.59	0.87	0.82	0.67
ORG2-BCOC_sm	−15	−12	6	10	0.69	0.81	0.84	0.66	0.70	0.86	0.78	0.48

Table 4. Summary of where a statistical improvement in the predicted number concentrations at the ground sites is achieved by including BL nucleation in the model. The results are given for particle number concentrations in three size ranges; D_{p} = 15–50 nm ($N_{<50}$), D_{p}>50 nm (N_{50}), and D_{p}>100 nm (N_{100}). The + sign indicates where the difference between the model and observations changes from statistically significant to not significant when BL nucleation is included. The – sign indicates where the reverse occurs i.e. including BL nucleation leads to an over prediction of the observed mean $N_{<50}$, N_{50}, or N_{100}. The 0 indicates where there is no statistically significant change in the predicted particle number concentrations with BL nucleation.

Ground site	$N_{<50}$	N_{50}	N_{100}
Aspvreten	+	+	+
Cabauw	0	0	0
Finokalia	+	+	0
Hohenpeissenberg	+	+	0
Hyytiälä	0	+	+
Jungfraujoch	0	0	0
JRC-Ispra	0	0	0
K-puszta	0	+	0
Košetice	0	0	0
Mace Head	0	0	0
Melpitz	0	0	0
Monte Cimone	+	+	+
Puy de Dôme	0	0	0
Schauinsland	+	+	–
Vavihill	+	0	+

Table 5. Summary statistics for particle number concentrations in the diameter ranges; 4–10 nm (N_{4-10}), 10–160 nm (N_{10-160}), and 160–1040 nm ($N_{160-1040}$). The normalised mean bias (NMB), slope of the linear regression (m) and correlation coefficient (R^2) are calculated between the simulated and observed mean number concentrations in the BL (≤ 2000 m a.s.l.) for each flight performed by the DLR Falcon aircraft during LONGREX, May 2008. R^2 and m are not calculated for N_{4-10} for reasons explained in Sect. 4.2. Values in brackets are statistics calculated with 1 flight (the second flight on 22 May) removed.

Model		NMB (%)		m		R^2	
Experiment	N_{4-10}	N_{10-160}	$N_{160-1040}$	N_{10-160}	$N_{160-1040}$	N_{10-160}	$N_{160-1040}$
BCOC_lg	−100	−85	−21	0.04	0.34	0.04	0.26
BCOC_sm	−100	−63	−22	0.17	0.31	0.21	0.14
ACT-BCOC_lg	−92	−59 (−83)	−19	−0.40 (0.02)	0.57	0.03	0.49
ACT-BCOC_sm	−95	−59 (−61)	−17	0.06 (0.08)	0.26	0.02	0.07
KIN-BCOC_lg	−38	−44 (−80)	−21	−0.64 (0.01)	0.27	0.03	0.11
KIN-BCOC_sm	−96	−56 (−60)	−22	0.06 (0.08)	0.25	0.02	0.08
ORG1-BCOC_lg	−71	−47 (−79)	−20	−0.58 (0.01)	0.51	0.03	0.41
ORG1-BCOC_sm	−80	−54 (−59)	−22	<0.03 (0.08)	0.22	<0.01	0.06
ORG2-BCOC_lg	−33	−59 (−79)	−24	−0.35 (0.02)	0.40	0.03	0.32
ORG2-BCOC_sm	−90	−56 (−61)	−17	0.01 (0.06)	0.16	<0.01	0.02

Table 6. Correlation coefficient (R^2) between observed and simulated hourly mean particle number concentrations **(a)** D_{p}>15 nm and **(b)** D_{p}>100 nm at each ground site. Ground site acronyms are given in Table 1.

(a) Model experiment	ASP	CBW	FKL	HPB	HTL	JFJ	JRC	KPO	KTC	MHD	MPZ	MTC	PDD	SLD	VHL
BCOC_hi	<0.01	0.30	0.05	0.13	0.01	0.16	0.09	0.09	0.02	0.04	<0.01	0.15	0.17	0.16	<0.01
BCOC_lo	<0.01	0.27	0.02	0.16	<0.01	0.20	0.03	0.08	<0.01	0.05	0.01	0.09	0.12	0.09	0.01
ACT-BCOC_hi	<0.01	0.31	0.02	0.09	<0.01	0.19	0.01	0.09	0.07	<0.01	0.03	0.02	0.01	0.05	<0.01
ACT-BCOC_lo	0.01	0.27	0.02	0.02	<0.01	0.21	0.01	0.08	0.04	0.03	0.01	<0.01	0.06	<0.01	<0.01
KIN-BCOC_hi	<0.01	0.26	0.01	0.09	<0.01	0.17	0.01	0.02	0.03	<0.01	0.02	0.02	<0.01	0.05	0.01
KIN-BCOC_lo	<0.01	0.27	0.01	0.04	<0.01	0.18	0.01	0.08	0.04	0.01	0.01	0.01	0.02	0.01	<0.01
ORG1-BCOC_hi	0.01	0.22	0.01	0.09	<0.01	0.06	<0.01	0.03	0.05	0.01	0.02	0.04	<0.01	0.07	0.06
ORG1-BCOC_lo	0.01	0.27	0.01	0.03	<0.01	0.10	<0.01	0.10	0.09	0.03	0.03	<0.01	0.02	0.01	0.02
ORG2-BCOC_hi	<0.01	0.30	0.02	0.09	<0.01	0.19	0.01	0.01	0.03	<0.01	0.01	0.02	<0.01	0.06	0.05
ORG2-BCOC_lo	<0.01	0.27	0.02	0.02	0.01	0.22	0.01	0.08	0.05	0.03	0.01	<0.01	0.04	0.01	0.01
(b) Model experiment	ASP	CBW	FKL	HPB	HTL	JFJ	JRC	KPO	KTC	MHD	MPZ	MTC	PDD	SLD	VHL
BCOC_hi	0.12	0.62	0.04	0.33	0.47	0.05	0.45	<0.01	0.19	0.34	0.17	0.34	0.30	0.22	0.32
BCOC_lo	0.13	0.48	0.02	0.37	0.43	0.08	0.42	<0.01	0.10	0.29	0.07	0.35	0.24	0.24	0.24
ACT-BCOC_hi	0.05	0.63	0.01	0.30	0.40	0.05	0.37	<0.01	0.18	0.31	0.20	0.33	0.30	0.20	0.30
ACT-BCOC_lo	0.09	0.47	0.02	0.35	0.42	0.07	0.41	<0.01	0.11	0.28	0.10	0.35	0.24	0.25	0.25
KIN-BCOC_hi	0.08	0.63	<0.01	0.30	0.42	0.05	0.35	<0.01	0.18	0.29	0.19	0.32	0.27	0.19	0.26
KIN-BCOC_lo	0.10	0.49	0.01	0.33	0.43	0.09	0.40	<0.01	0.11	0.27	0.07	0.34	0.23	0.25	0.24
ORG1-BCOC_hi	0.09	0.61	0.01	0.29	0.38	0.05	0.33	0.01	0.16	0.27	0.17	0.32	0.27	0.20	0.23
ORG1-BCOC_lo	0.12	0.49	0.01	0.34	0.45	0.08	0.37	0.01	0.09	0.27	0.09	0.34	0.26	0.26	0.25
ORG2-BCOC_hi	0.06	0.61	0.02	0.30	0.41	0.05	0.34	<0.01	0.18	0.30	0.18	0.32	0.27	0.20	0.28
ORG2-BCOC_lo	0.10	0.48	0.02	0.33	0.44	0.06	0.41	<0.01	0.11	0.27	0.07	0.35	0.25	0.26	0.26

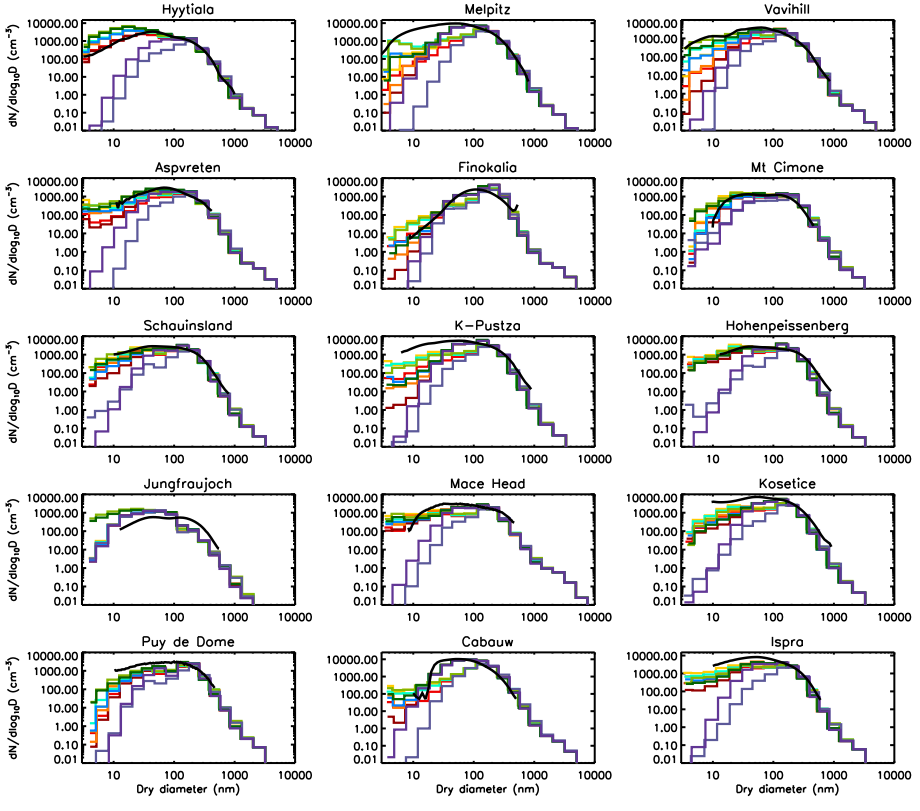

Fig. 3. Campaign-mean simulated (colour) and observed (black) total number size distributions at each ground site. Model experiments are described in Table 2: BCOC_lg (grey/blue), BCOC_sm (purple), ACT-BCOC_lg (red), ACT-BCOC_sm (maroon), KIN-BCOC_lg (yellow), KIN-BCOC_sm (orange), ORG1-BCOC_lg (light green), ORG1-BCOC_sm (dark green), ORG2-BCOC_lg (cyan), and ORG2-BCOC_sm (blue).

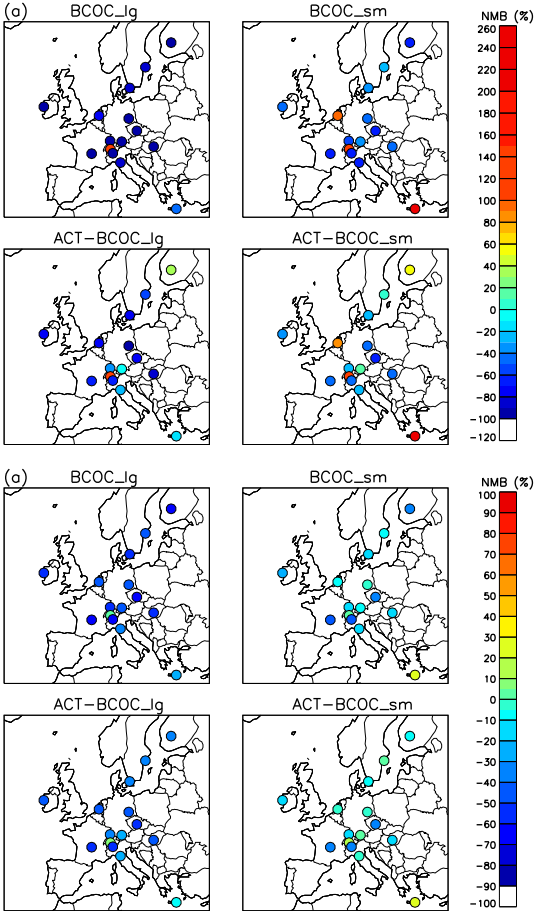

Fig. 4. Normalised mean bias (NMB) between hourly-mean modelled and observed particle number concentrations at each ground site. NMB is shown for model experiments 1–4, Table 2 for number concentrations in the size ranges; **(a)** $D_{\mathrm{p}} = 15$–50 nm and **(b)** $D_{\mathrm{p}} > 50$ nm.

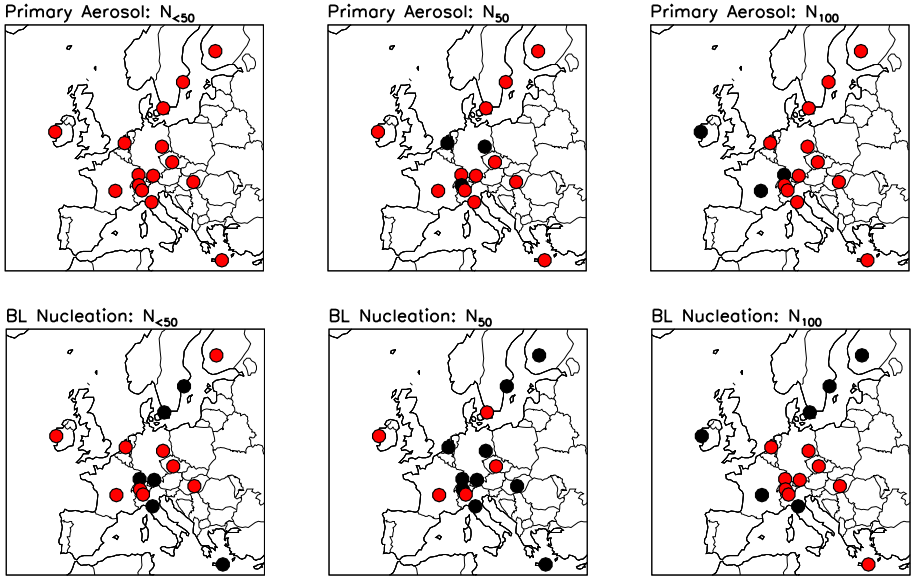

Fig. 5. Statistical significance between hourly-mean modelled and observed particle number concentrations in three size ranges; $D_{\mathrm{p}} = 15$–50 nm ($N_{<50}$), $D_{\mathrm{p}} > 50$ nm (N_{50}), and $D_{\mathrm{p}} > 100$ nm (N_{100}). The red dots show site locations where the difference between the model and observations is statistically significant at the 99 % confidence level; the black dots show the locations where the difference is insignificant. Results are shown for the primary aerosol model experiments (1–2, Table 2) and for the experiments including BL nucleation (3–10, Table 2).

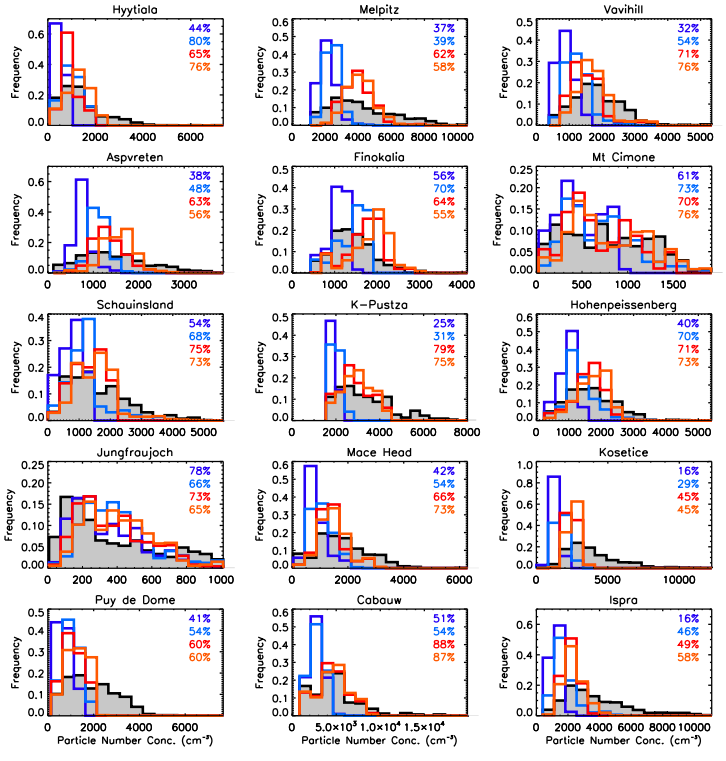

Fig. 6. Normalised histograms of the frequency distribution of hourly-mean simulated (colour) and observed (black) number concentrations of particles >50 nm (N_{50}) for May 2008 at each ground site. Bin size depends on the maximum N_{50} observed at each site, number concentrations are divided into 15 equally spaced bins. Model experiments are described in Table 2: BCOC_lg (blue), KIN-BCOC_lg (light blue), BCOC_sm (red), and KIN-BCOC_sm (orange). The percentage overlap of the modelled and observed frequency distributions is shown for each model simulation.

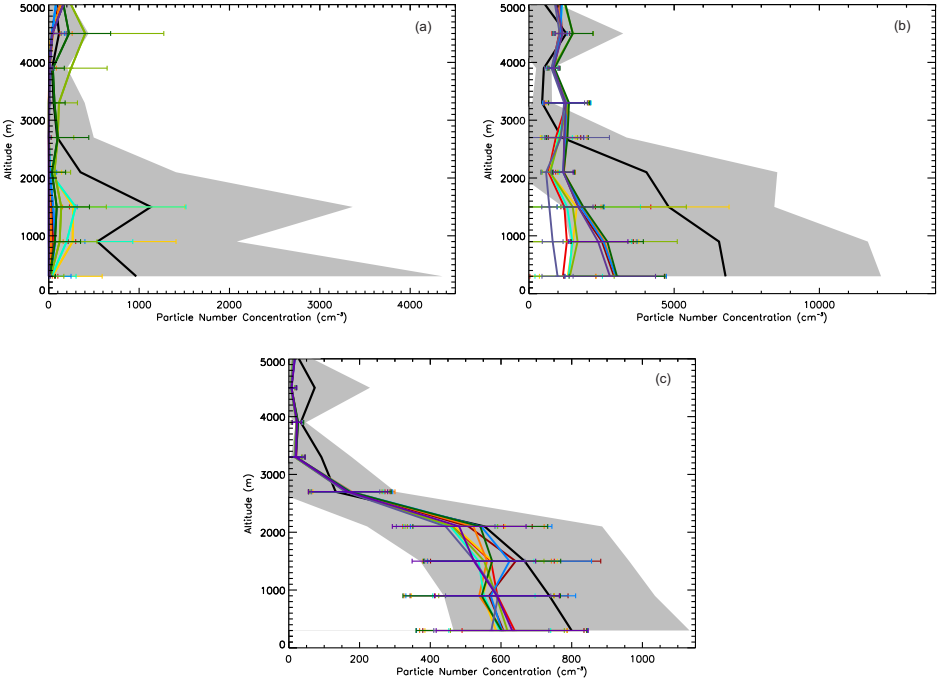

Fig. 7. Vertical profiles of observed (black) and modelled (colour) particle number concentrations in the diameter ranges: **(a)** 4–10 nm, **(b)** 10–160 nm, and **(c)** 160–1040 nm. Observations are from the DLR Falcon 20 aircraft. The average over all measurement flights performed during the LONGREX campaign (May 2008) is shown (sectioned into 600 m altitude bins). The error bars and shading represent the standard deviation of the model and observations, respectively. Model experiments are described in Table 2: BCOC_lg (blue/grey), BCOC_sm (purple), ACT-BCOC_lg (red), ACT-BCOC_sm (maroon), KIN-BCOC_lg (yellow), KIN-BCOC_sm (orange), ORG1-BCOC_lg (light green), ORG1-BCOC_sm (dark green), ORG2-BCOC_lg (cyan), and ORG2-BCOC_sm (blue).

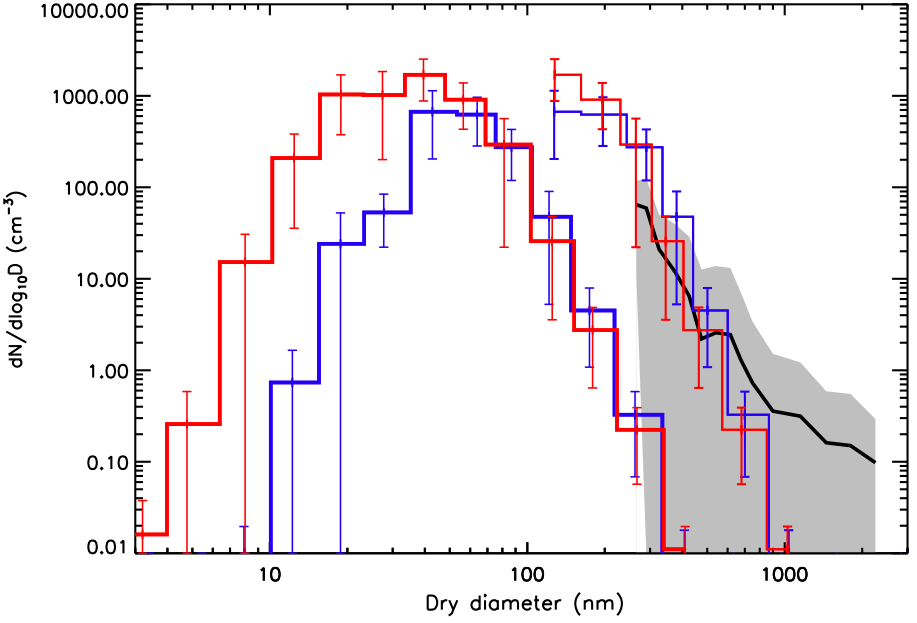

Fig. 9. Mean number size distributions of measured non-volatile particles (black) and of modelled carbonaceous particles (colour) for all flight hours with a mean altitude less than 2 km a.s.l. The total modelled size distribution of BC particle cores is shown in bold and the modelled size distribution of aged BC+OC (with condensed SO_4) is shown for sizes larger than $\sim$100 nm. The error bars and shading represent the standard deviation of the model and observations, respectively. Model experiments are described in Table 2: BCOC_lg (blue) and BCOC_sm (red).

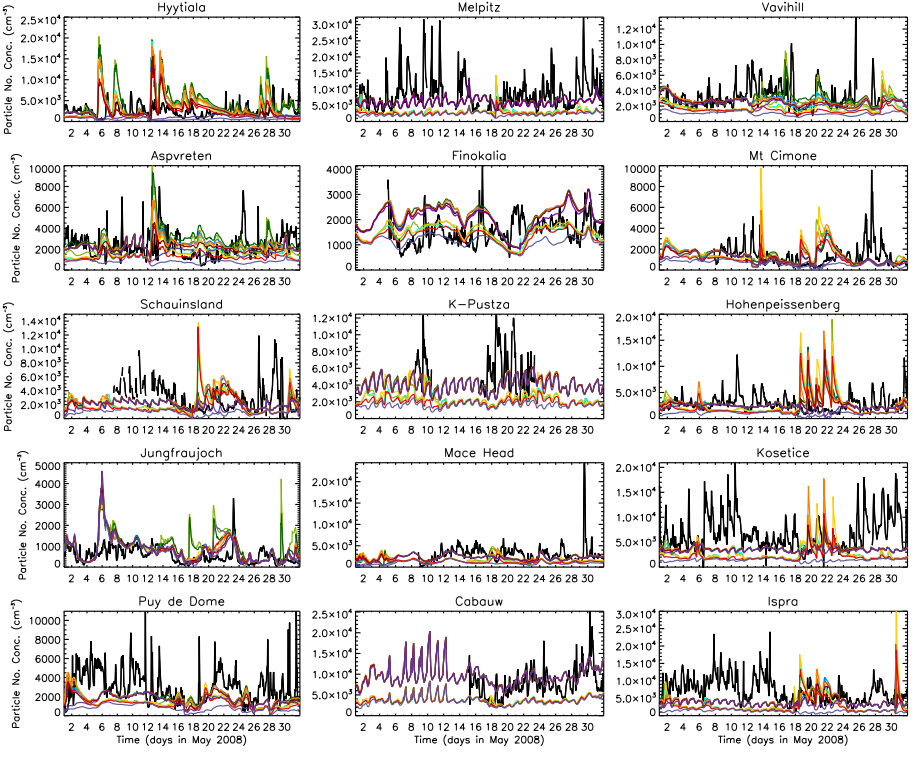

Fig. 10. May 2008 time-series of hourly-mean modelled (colour) and observed (black) particle number concentrations (D_p>15 nm) at each ground site. Model experiments are described in Table 2: BCOC_lg (grey/blue), BCOC_sm (purple), ACT-BCOC_lg (red), ACT-BCOC_sm (maroon), KIN-BCOC_lg (yellow), KIN-BCOC_sm (orange), ORG1-BCOC_lg (light green), ORG1-BCOC_sm (dark green), ORG2-BCOC_lg (cyan), and ORG2-BCOC_sm (blue).

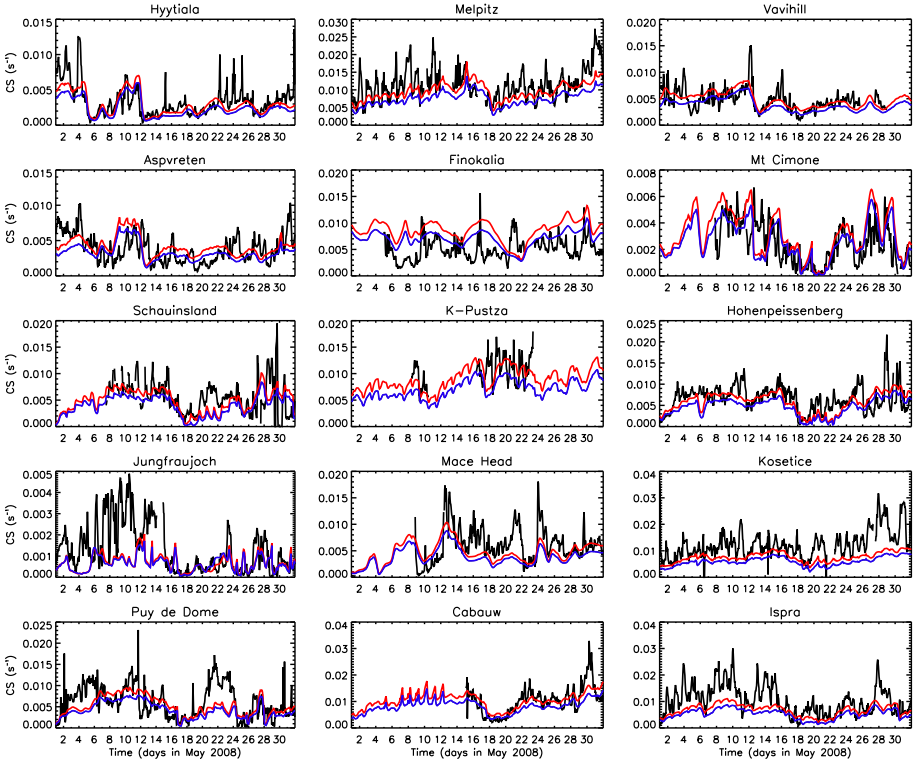

Fig. 11. May 2008 time-series of hourly-mean simulated (colour) and observed (black) condensation sink at each ground site. Model experiments are described in Table 2: BCOC_lg (blue) and BCOC_sm (red).